Temporal characterization of tunable EUV pulses in the sub-optical-cycle regime with FROGCRAB

Isabell Thomann, Emily Gregonis, Arvinder S. Sandhu, Margaret M. Murnane, Henry C. Kapteyn

JILA, University of Colorado and NIST, Boulder, Colorado 80309-0440, USA

E-mail: Isabell.Thomann@Colorado.edu

We temporally characterize sub-optical-cycle extreme-ultraviolet pulses using two-color cross-correlation. In this regime intermediate between the generation of a single attosecond burst and attosecond pulse trains, we show that careful application of the FROGCRAB technique through a progressive fitting procedure allows for the determination of the EUV pulsewidth without the need for deconvolution from the driving laser. We characterize an EUV pulse consisting of ~ 470 attosecond bursts with a <1.5 fs FWHM intensity envelope. Although the FROGCRAB technique uses a seemingly complex phase modulation gate, considerable intuition about the EUV pulse characteristics can be obtained.

4265Ky, 4265Re, 4250Hz, 7847+p

High-order harmonic upconversion of intense femtosecond laser pulses provides a tabletop-scale source of coherent light in the extreme ultraviolet (EUV) region of the spectrum. This source has produced the shortest light pulses measured to-date, making it ideal for studies of dynamic processes in the femtosecond (fs= 10^{-15} s) to attosecond (as= 10^{-18} s) regime. In general, high-order harmonic generation (HHG) produces a train of attosecond bursts, with an interpulse spacing corresponding to half of the driving pulse period. Under specific conditions, either trains of attosecond pulses, or isolated attosecond bursts, can be produced.[1-5] To date, individual attosecond pulses as short as 130 as have been generated and measured using very short, 5 fs, carrier-envelope-phase stabilized driving laser pulses [5]. However, many experiments in molecular and materials spectroscopy require EUV pulses slightly longer in duration, in the range of ~1 fs.[6] Provided these pulses are near the Fourier-transform limit in pulse duration, and thus have a correspondingly narrow spectral bandwidth, specific states can be accessed with reasonable spectroscopic resolution (~1 eV). The generation and characterization of pulses with these characteristics is a heretofore unexplored topic of great interest.

One of the major stumbling blocks in this area is in characterizing light pulses with duration in the range of ~1-2 fs. Nearly all current EUV pulse characterization techniques rely on two-color EUV/near infrared photoionization. In the case of relatively long EUV pulses, the EUV duration can be deconvolved provided the NIR pulse duration is accurately characterized, and the RABBITT (Reconstruction of Attosecond Beating by Interference of Two-photon Transitions) technique [9] can be used to determine the temporal structure of the individual attosecond bursts. However, a direct envelope deconvolution becomes increasingly inaccurate when the EUV pulse duration is much shorter than the NIR, and RABBITT only determines the time structure of individual attosecond bursts but not the overall envelope. The FROGCRAB

(Frequency-Resolved Optical Gating for Complete Reconstruction of Attosecond Bursts) technique, has recently been introduced [11]; this technique is a generalization of previous techniques, which allows for reliable deconvolution of EUV pulses of any duration. However, FROGCRAG has to-date been applied only to the case of a single isolated EUV burst of 130 as duration [5], where the time-frequency structure of the FROGCRAB trace simplifies considerably.

In this work we exploit the full potential of FROGCRAB for the first time by applying it to a complex EUV field in the challenging regime intermediate between a single isolated attosecond pulse and a long attosecond pulse train. Furtermore, this work presents the first detailed temporal characterization of high harmonic light generated in a hollow waveguide geometry. We report on the generation and temporal characterization of sub-optical-cycle EUV pulses with a measured FWHM (full-width at half maximum) intensity envelope of < 1.5 fs. These pulses are generated using 13 fs driving laser pulses focused into a gas-filled waveguide, without the need for stabilizing the carrier wave with respect to the pulse envelope. The radiation is spectrally relatively narrow (~64 % of the energy is contained in a single 1.1 eV harmonic peak) and energy-tunable from the 23rd harmonic to the 29th harmonic by adjusting the fundamental laser intensity and gas pressure in the waveguide. By application of the FROGCRAB technique, we measure the EUV pulse to consist of three ~ 470 attosecond bursts in a <1.5 fs FWHM intensity envelope. To fit the experimental data, we use a step-by-step procedure to obtain the chirp of the individual bursts as well as the overall pulsewidth from the FROGCRAB data, resulting in excellent agreement between the data and the reconstruction, with minimal iteration and without the need for deconvolution from the driving laser. This work demonstrates how interferometric EUV-visible cross correlation data, when analyzed carefully, can be used to characterize pulses of short, intermediate, and long pulse duration.

To temporally characterize the EUV pulse, we employ an interferometric EUV – IR cross correlation geometry first introduced in [8]. Both beams are focused into a Helium gas jet, and a cross-correlation signal is obtained from the generated photoelectron spectra as the relative delay between the two pulses is varied. The delay line makes use of the different divergences of the fundamental and the EUV beam. The low divergence, central EUV beam passes through a small circular Al filter suspended in a nitrocellulose filter. The annular fundamental beam, which passes around the Al filter, is reflected by an annular mirror, while the central EUV beam is reflected by a Mo/Si mirror that is mounted on a piezoelectric transducer to introduce a variable delay between the fundamental beam and the EUV beam. The Mo/Si mirror reflectivity is centered at ~ 47 eV with a FWHM ~13 eV, so that all generated harmonics are reflected. The photoelectrons ejected from Helium by the EUV beam are then detected using a magnetic bottle time-of-flight spectrometer and a multichannel plate (MCP) detector. This spectrometer has a 2-Pi detection solid angle i.e. photoelectrons parallel and perpendicular to the laser polarization (which points towards the MCP) are detected.

Figure 1(a) shows the experimental cross-correlation data. At large time delays between the EUV and IR pulses, the photoelectron spectra are generated by the EUV light alone. The photoelectron peak generated by the dominant harmonic is clearly visible, as well as two adjacent smaller photoelectron peaks generated by the two adjacent weaker harmonics. When both EUV and fundamental beams are present, sidebands occur due to the absorption of an EUV photon simultaneous with absorption or emission of a fundamental photon. The sidebands are modulated at a period corresponding to half the fundamental laser cycle. Fig. 1(c) shows a cosine fit to the photoelectron sideband that lies between harmonics 29 and 31, described by the interference term $\cos(2*\omega_L*\tau+ \varphi_{q-1}- \varphi_{q+1}+ \Delta\varphi^f_{atomic})$, where ω_L is the fundamental laser frequency, τ the delay between EUV and fundamental field, $\varphi_{q-1}$and φ_{q+1} the adjacent harmonic phases and $\Delta \varphi^f_{atomic}$ is the atomic phase at the final state [9].

In the following, we use the FROGCRAB technique for a careful analysis of our data. FROGCRAB is based on the well-established FROG technique for measuring ultrashort laser pulses in the IR/visible region, where a temporal gate is used to measure the spectrum of each temporal slice [10]. The temporal gate for FROG is usually an amplitude gate. Instead of an amplitude gate, FROGCRAB uses the fundamental field as a phase gate that modulates the electron wavepacket ionized by the EUV beam. It is established that for most conventional FROG techniques [10], spectrograms will have a certain shape depending on the phase of the E-field to be measured. One might expect that the phase-gate used in FROGCRAB might generate less-intuitive traces [11]. However, as we show below, this is not the case.

To generate simulated FROGCRAB traces, we employed the strong-field-approximation expression given in [11]. We adapted it to our experimental case where photoelectrons are detected over a 2-π solid angle, by averaging the photoelectron distribution for different angles including both a geometrical weighting as well as the differential partial cross section for detecting photoelectrons from Helium. Our FROGCRAB trace is the addition of two traces for the fundamental light, a cosine and minus cosine waveform. The reason is that we do not need phase stabilized laser pulses, and the conditions for generating high harmonics (phase-matching and recollision) are the same for both waveforms. For each delay step, photoelectrons are acquired for multiple laser shots, and therefore can contain signal from both waveforms.

Before turning to a detailed analysis of our EUV radiation using FROGCRAB, we first show that, although FROGCRAB uses a seemingly complex phase modulation gate, considerable intuition about pulse characteristics can be obtained from the shape of the sidebands. To demonstrate this, we apply individual dispersion orders to artificially constructed EUV bursts, similar to those generated in our experiment. Sample results of FROGCRAB traces are shown in Fig. 2, plotted over a delay range of two fundamental laser cycles. Figures 2(a) – 2 (c) show that the shape of the sidebands change significantly depending on whether 2^{nd} order phase D2 (Fig. 2(a)), 3^{rd} order phase D3 (Fig. 2(b)) or 4^{th} order phase D4 (Fig. 2(c)) is added. FROGCRAB traces can also indicate the sign of the dispersion order, because for opposite signs of dispersion, the sidebands are inverted along the time delay axis.

We now turn to a detailed analysis of our experimental FROGCRAB data. To construct the EUV electric field for the simulated FROGCRAB trace, we start with the EUV spectrum shown in Fig. 1 (b), recorded using an x-ray spectrometer and CCD. This EUV spectrum is then deconvolved with the Gaussian spectrometer resolution function of 0.38 eV FWHM, determined by a separate measurement using spectrally narrow harmonics. (Using the measured EUV spectrum without deconvolution would underestimate the pulse duration by ~5%). The deconvolved EUV spectrum is then multiplied by the transfer functions that relate the measured EUV spectrum to that incident on the detection gas. A spectral phase, described below, is added to the EUV spectrum $E(\omega)$, before transforming into the time domain. The calculated FROGCRAB trace is finally convolved with the measured photoelectron spectrometer resolution function of width $\Delta E = 0.726$ eV. This photoelectron spectrometer resolution ΔE imposes an upper limit of approximately $h*0.44/\Delta E$ on the envelope duration that can reliably be measured. With the current resolution, we can characterize pulse durations up to 2.5 femtoseconds.

As shown above, we can retrieve higher order spectral phases with FROGCRAB. Therefore, in Fig. 3(a), we vary the 2^{nd} order phase and compare the RMS deviation of the experimental and calculated FROGCRAB trace. We obtain a 2^{nd} order phase of D2 = -0.0325 fs^2. Using the same procedure we obtain a minimum RMS deviation for third order dispersion at D3 = -0.00675 fs^3 in Fig. 3(b). The atomic phase of the detection gas, as well as contributions from the EUV mirror and the Al filters, are negligible at the EUV energies considered. Using the best values for the second and third order dispersions found in this way, we construct the simulated FROGCRAB trace, shown in Fig. 3(d). This agrees very well and in detail with the experimental trace in Fig. 3(e). The full simulated FROGCRAB trace is shown in Fig. 3(f), and compares excellently with the experimental trace shown in Fig. 3(g).

With the above analysis, we can now plot the correct chirped EUV electric field envelope, shown in black in Fig. 4(a). For comparison, the transform-limited electric field envelope is also shown in grey. Figure 4(b) shows the intensity versus time of the chirped EUV pulse (black), as well as the envelope corresponding to the transform-limited center harmonic for comparison (dashed grey line). Figure 4 shows that the attosecond bursts are broadened from their transform-limited value of 360 attoseconds, to a chirped value of 470 attoseconds, while the total EUV radiation is contained in an overall intensity envelope of 1.4 +/- 0.2 fs FWHM. This corresponds to a single burst with two <10% sidelobes in the case of a cosine pulse. However, distinguishing a cosine from a sine pulse with two equivalent intensity bursts (shown in solid grey in Fig. 4(b)) is not possible. This is because the two FROGCRAB traces are equivalent. To validate the FWHM EUV envelope extracted from our analysis, we also explored the effect of varying the envelope duration in our simulated FROGCRAB traces. We found that varying the pulse envelope also changes the widths and the shape of the FROGCRAB sidebands. A plot of the RMS deviation between the simulated and experimental FROGCRAB traces versus FWHM EUV pulse duration is shown in Fig. 3(c). It can be seen that the best agreement is found for a FWHM EUV pulse duration of 1.44 fs, in very good agreement with the duration of the EUV field reconstructed from the CCD spectrum for dispersions of D2 = -0.0325 fs^2 and D3 = -0.00675 fs^3. We verified that deconvolution from the fundamental laser pulse is unnecessary for retrieving the correct EUV pulse structure, by only using the central two fundamental cycles of the FROGCRAB trace and (a) setting the fundamental pulse duration to infinity, and (b) varying the fundamental wavelength between 700 nm and 830 nm.

The FWHM duration of the measured cross correlation data shown in Fig. 3(g) is 13 fs, which agrees well with the laser pulse duration measured independently using a Grenouille device. A non-interferometric cross-correlation measurement would be suitable for EUV pulses on the order of 10 fs, but would fail to accurately characterize EUV pulse durations of 1-2 fs, because the measured cross-correlation width would be dominated by the fundamental laser pulse. To determine the exact duration of our EUV pulses from a simple cross correlation measurement, both the laser pulse and the cross correlation would need to be measured with an accuracy better than ~ 0.05 fs in order to accurately determine the pulse duration of the EUV radiation. Thus for the EUV pulse durations investigated here, the correct duration can only be found by analyzing the shape and width of the sidebands.

Finally, this work also significantly expands on previous spectral measurements and models reported in [6], which first observed a new phase matching regime in a waveguide when HHG is driven by ≈ 10 fs laser pulses. In that work, bright, sub-optical cycle, quasi-monochromatic and tunable EUV light was generated via a new non-linear stabilization mechanism, and phase-matched EUV emission was predicted to be localized to within a sub-optical cycle. Calculations have predicted that this should result in relatively short-duration pulses where the pulse shape is relatively insensitive to carrier-envelope phase. This prediction is in agreement with our measurements.

In conclusion, we have demonstrated that the FROGCRAB technique can be successfully used to bridge the gap in EUV pulse measurement capabilities between simple noninterferometric crosscorrelation measurements (which are suitable for EUV pulses of ~10 fs) and RABBITT, which determines the time structure of individual attosecond bursts but not the overall envelope. Using FROGCRAB, we have temporally characterized EUV pulses with an intensity envelope of 1.4 fs and individual chirped bursts of 465 attoseconds. These short pulses are energy-tunable between the 23rd and 29th harmonics, and are obtained without the use of very short driving pulses or CEP stabilization. Both the simplified generation scheme and the flexible tunability of this radiation greatly facilitate time resolved experiments using sub-optical-cycle EUV pump or probe pulses, making it potentially extremely useful for studies of fast dynamics in molecules and materials. We also showed that considerable intuition on EUV pulse characteristics can be obtained from the FROGCRAB trace, and that it can be used to extract higher order spectral phase contributions as well as the overall EUV intensity envelope. FROGCRAB is thus suitable to characterize pulses with a sub-optical-cycle envelope and will be a useful tool to characterize other complicated attosecond-structure fields.

We gratefully acknowledge support for this work from the National Science Foundation Physics Frontier Centers Program. We also thank Farhad Salmassi, Andy Aquila and Yanwei Liu for fabricating the EUV mirror.

References

[1] Rodrigo Lopez-Martens et al., Phys. Rev. Lett. 94, 033001 (2005).

[2] Ivan P. Christov et al., Phys. Rev. Lett. 78, 1251 (1997).

[3] R. Kienberger et al., Nature 472, 817 (2004).

[4] P. B. Corkum et al., Opt. Lett. 19, 1870 (1994).

[5] G. Sansone et al., Science 314, 443 (2006).

[6] Arvinder S. Sandhu et al., Phys. Rev. A 74, 061803 (2006).

[7] A. Rundquist et al., Science 280, 1412 (1998).

[8] M. Drescher et al., Science 291, 1923 (2001).

[9] P. M. Paul et al., Science 292, 1689 (2001).

[10] R. Trebino, Frequency-Resolved Optical Gating: The Measurement of Ultrashort Laser Pulses, Kluwer Academic Publishers, Boston (2000).

[11] Y. Mairesse et al., Phys. Rev. A 71, 011401 (2005); F. Quere et al., Journal of Modern Optics 52, 339 (2005).

Figure Captions

FIG. 1. (a) Experimental photoelectron spectrum as a function of time delay between the EUV and IR pulses, when these pulses are focused simultaneously into He gas. (b) Experimental CCD spectrum of the EUV radiation that generated the photoelectron spectrum shown in (a). The energy tuning range is indicated. (c) Oscillatory sideband signal at harmonic order 30 from the data shown in (a), as a function of time delay between the EUV and IR pulses (black), and cosine fit (grey).

FIG. 2. Simulated FROG-CRAB data, when higher dispersion orders are artificially introduced into the EUV field: (a) 2^{nd} order D2, (b) 3^{rd} order D3, (c) 4^{th} order D4. Intuitively the sideband shape shows the group delay $\tau = d\phi(\omega)/d\omega =$ h/(2 pi) $d\phi$(Energy)/dEnergy of the EUV radiation, as indicated by black lines.

FIG. 3. RMS deviation between the FROG-CRAB simulation and the experimental cross-correlation trace as the parameters of the simulated pulse are varied: (a) Varying the linear chirp D2, (b) Varying the quadratic chirp D3, (c) Varying the EUV pulse envelope. (d, f) FROGCRAB data simulated using the optimized values of D2, D3 and the EUV pulse envelope, (e, g) experimental FROGCRAB data.

FIG. 4. (a) (Black) Extracted chirped EUV electric field envelope vs. time; (grey) transform limited pulse for comparison. (b) (solid black) Extracted EUV intensity vs. time corresponding to the chirped pulse shown in (a); (solid grey) intensity of a double pulse with the same envelope; (dashed grey) intensity envelope of the extracted EUV field.

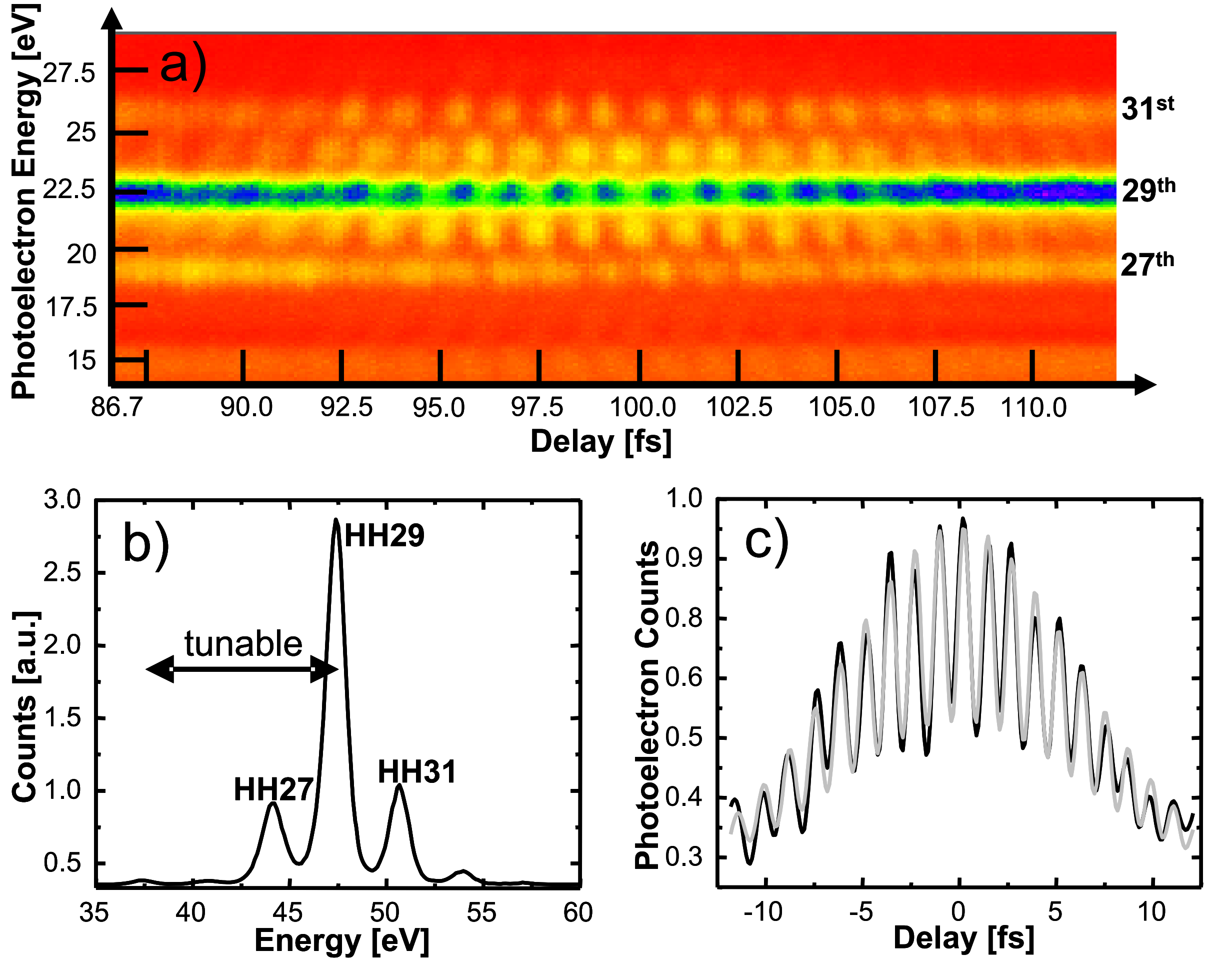
a)
Photoelectron Energy [eV]
27.5
25
22.5
20
17.5
15
31st
29th
27th
86.7
90.0
92.5
95.0
97.5
100.0
102.5
105.0
107.5
110.0
Delay [fs]
b)
Counts [a.u.]
3.0
2.5
2.0
1.5
1.0
0.5
tunable
HH29
HH27
HH31
35
40
45
50
55
60
Energy [eV]
c)
Photoelectron Counts
1.0
0.9
0.8
0.7
0.6
0.5
0.4
0.3
-10
-5
0
5
10
Delay [fs]

FIGURE 1

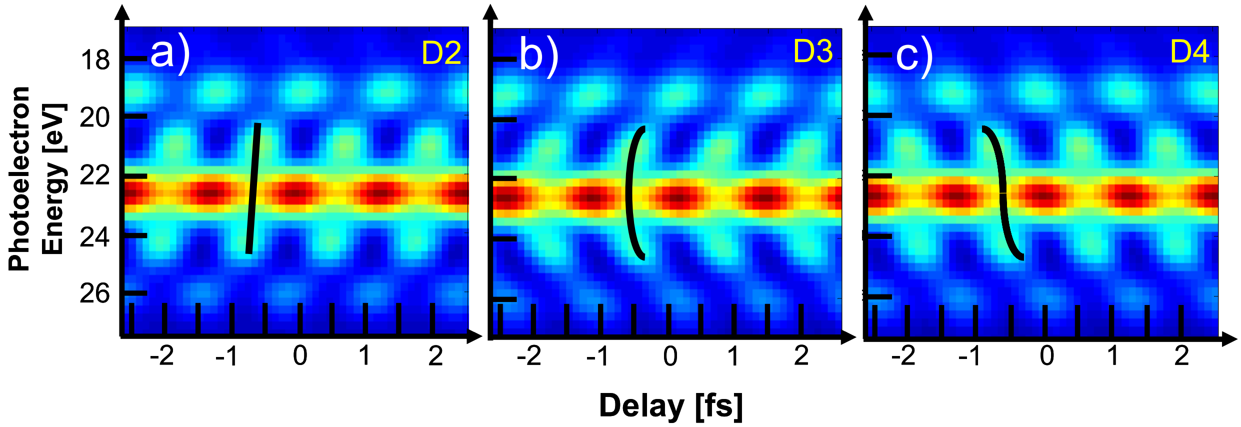
a)
D2
b)
D3
c)
D4
Photoelectron Energy [eV]
18
20
22
24
26
-2
-1
0
1
2
Delay [fs]

FIGURE 2

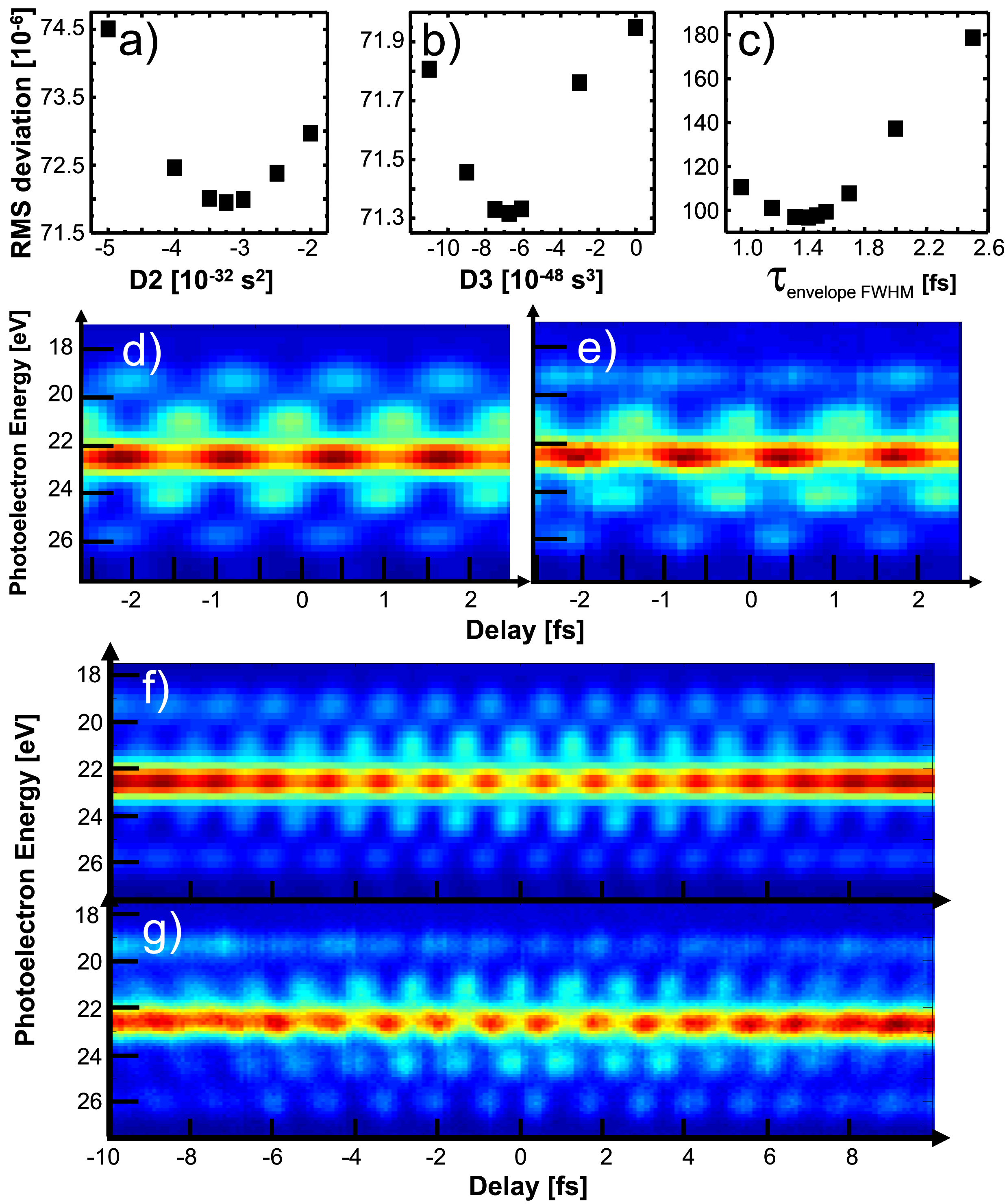
a)
b)
c)
d)
e)
f)
g)
RMS deviation [10^-6]
D2 [10^-32 s^2]
D3 [10^-48 s^3]
τ envelope FWHM [fs]
Photoelectron Energy [eV]
Delay [fs]

FIGURE 3

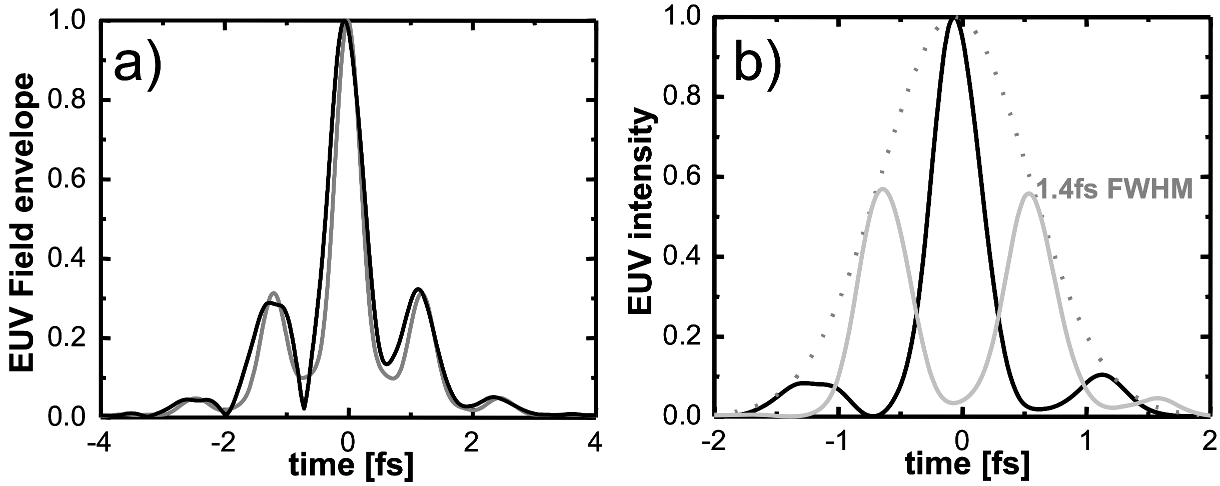

a)
EUV Field envelope
1.0
0.8
0.6
0.4
0.2
0.0
-4
-2
0
2
4
time [fs]
b)
EUV intensity
1.4fs FWHM
-2
-1
0
1
2
time [fs]

FIGURE 4